Zhang *et al.*
Chinese Journal of Mechanical Engineering (2023) 36:16
https://doi.org/10.1186/s10033-023-00852-2

Chinese Journal of Mechanical Engineering

ORIGINAL ARTICLE

Open Access

Local Buckling-Induced Forming Method to Produce Metal Bellows

Tianyin Zhang[1], Dongqing Li[2], Tianjiao Xu[1], Yongfeng Sui[2] and Xianhong Han[1,3*]

Abstract

A novel buckling-induced forming method is proposed to produce metal bellows. The tube billet is firstly treated by local heating and cooling, and the axial loading is applied on both ends of the tube, then the buckling occurs at the designated position and forms a convolution. In this paper, a forming apparatus is designed and developed to produce both discontinuous and continuous bellows of 304 stainless steel, and their characteristics are discussed respectively. Furthermore, the influences of process parameters and geometric parameters on the final convolution profile are deeply studied based on FEM analysis. The results suggest that the steel bellows fabricated by the presented buckling-induced forming method have a uniform shape and no obvious reduction of wall thickness. Meanwhile, the forming force required in the process is quite small.

Keywords Buckling-induced forming, Dieless, No wall-thinning, Stainless-steel bellows

1 Introduction

The purpose of this paper is to develop a dieless forming method for metal bellows based on controllable buckling deformation.

Metal bellows are thin-walled axisymmetric shells composed of a series of ring-shaped convolutions, which have the flexibility to absorb irregular expansion and contraction caused by axial force, external pressure and bending moments in the piping system [1]. Metal bellows usually possess higher pressure and buffer capacity than ordinary straight pipes, especially in the working conditions of the forced axial and bending displacement [2, 3]. They have been widely applied as expansion joints, flexible connectors, pressure relief valves and energy-absorbing components in vacuum systems, aerospace industries, micro-electromechanical systems, etc., playing an important role in weight reduction, strength improvement and energy absorption [4].

The hydroforming process and the mechanical forming process are two of the most widely used approaches to fabricating metal bellows [5]. Lee [6] applied the finite element method (FEM) and the Taguchi method to analyze the influence of hydroforming parameters such as wall thickness, internal pressure and die stroke on the convolution contour, among which the die stroke is the biggest influencing factor on determining the final shape. Faraji et al. [7] analyzed the effects of internal pressure, die stroke, axial feeding and material property on thickness distribution, crown diameter and spring back. It was observed that an increase in axial feeding, die stroke and internal pressure leads to excessive thinning. Zhan et al. [8] proposed a mandreless neck-spinning forming process to produce both single and double corrugated cylindrical parts successfully, and they also found that the small roller fillet radius and big feed rate lead to poor geometric accuracy. Shi et al. [9] proposed an internal spinning incremental forming technology for metal bellows by combining incremental forming technology with

*Correspondence:
Xianhong Han
hanxh@sjtu.edu.cn
[1] Institute of Forming Technology & Equipment, School of Materials Science and Engineering, Shanghai Jiao Tong University, Shanghai 200030, China
[2] Hangzhou Steam Turbine & Power Group Co., Ltd, Hangzhou 310100, China
[3] National Engineering Research Center of Die and Mold CAD, Shanghai Jiao Tong University, Shanghai 200030, China

a tube spinning forming process. The tube wall in the transition region of the arc and the tensile region of the inclined plane is prone to produce excessive deformation and crack. The prementioned approaches have some deficiencies. The hydroforming process generally requires expensive tools and complicated sealing modules, which is not efficient for small-batch manufacturing. And the mechanical forming process normally forms the convolutions through the contact force between the tool and the tube, which decreases the surface quality of bellows. Some other forming technologies have also been used to produce metal bellows, such as rubber-pad forming, electric-assisted forming [10], viscous medium pressure forming [11], etc. It is noted that most of the prementioned forming methods cause the wall thinning since the deformation area of the tube billet is mainly under a tensile stress state, which induces a high risk of cracking during the forming process and significantly affects the subsequent service life.

When the plates or shells are subjected to the compression load within the plane, if the load reaches the critical value, the structures will suddenly produce out-of-plane deformation, which is called buckling. Traditionally, buckling is regarded as a failure mode and should be avoided in structural design and manufacturing. However, the rational utilization of buckling instability is a burgeoning trend recently, which even gained a dedicated name of Buckliphilia [12].

In terms of buckling application on mechanism design, Borchani et al. [13] investigated the control of snap-through events by using buckled beam elements to generate high-rate excitations for piezoelectric transducers. Erbil et al. [14] developed an all-electrostatic architecture composed of efficient actuators and multiplexed shape-shifting devices to control the compressive force, as well as the direction and degree of buckling. Based on the ancient arts of origami/kirigami, Zhao et al. [15] developed three-dimensional morphable mesostructures through local controllable buckling and twisting, which has great application potential in the field of flexible electronics. In terms of buckling application in manufacturing, Yuan et al. [16] introduced useful wrinkles by axial loading before tube hydroforming, which can effectively improve the formability of tubes. Alves et al. [17] developed an innovative tube connection technology by using the convolutions produced by local buckling of thin-walled tubes, which led to significant economic and time savings. Supriadi et al. [18] developed a semi-dieless metal bellow forming method with a local induction heating technique in which a mandrel was inserted into the metal tube. They also studied the effect of compression ratio and wall thickness on the bellows' characteristics. Based on this principle, Furushima et al. [19] proposed a two-step method to further increase the convolution height and obtained a quite stable bellow shape. Zhang et al. [20] manufactured the aluminum alloy bellows, confirming that the semi-dieless metal bellow forming process is applicable to materials with high thermal conductive coefficients. Sedighi et al. [21] produced metal bellows with local electric arc heating and axial compression. The influence of compression stroke and working current on the forming force, the convolution height, as well as the wall thickness, were investigated. Actually, buckling deformation makes the material mainly in a compressive stress state, thus the wall thickness is usually not reduced but increased, which is quite attractive because the common forming methods such as hydroforming usually have a thinning rate of 20–30% [22, 23].

The motivation of this paper is to introduce the idea of controllable buckling into the metal bellow forming, where the thermal buckling-induced forming process involving local induction heating and axial compression is proposed. Concretely, an experimental forming apparatus is developed and two forming modes can be chosen to produce the SUS304 stainless-steel bellows. The forming apparatus does not require dies or sealing modules, which avoids the surface defects of bellows caused by mechanical friction and reduces production costs. Furthermore, the effects of forming parameters on deformation characteristics are investigated with the help of finite element analysis.

2 Forming Apparatus and Process

2.1 Forming Apparatus

2.1.1 Design Principle

The thermal buckling-induced forming process of metal bellows described in this paper is based on the buckling behavior of the material in the softening region when subjected to axial compression, so it is necessary to form a gradient property distribution along the tube through rapid heating and cooling. The joint control of heating and cooling sources makes the high temperature distributed in the local target region, where the material has lower bending stiffness because the high temperature reduces the effective tangent modulus. When the tube is subjected to compression loading, a quite small force can cause local instability of the low stiffness region. And the increase in deflection, as a geometric factor, further reduces the bending stiffness of the deformation zone and eventually leads to the formation of a single target convolution. Actually, the thermal buckling-induced forming process is a typical strain-path change behavior. And the plastic flow of material in this condition is quite complicated and usually does not follow the associated flow rule. More details can be found in Ref. [24].

Figure 1(a) shows the schematic illustration of the thermal buckling forming apparatus for metal bellows. With the combination of induction heating and annular air jet cooling, the temperature of a local area (called deformation area) rises to a certain value that diminishes the flow stress of the material. After that, the different moving speeds of the two ends ($V_2 > V_1$) induce an axial compression force, leading to an outward axisymmetric buckling deformation to form a convolution. When the formed convolution moves to the cooling region, its strength and stiffness increase rapidly, which prevents further plastic deformation. At the same time, the temperature of the adjacent area is elevated by the heating source. With the cycle of the above operations, a high-quality metal bellow of no obvious wall-thinning is fabricated.

Based on the prementioned design principle, an experimental forming apparatus with a dimension of 2.5 m×1.2 m×1.5 m has been produced, the schematic diagrams of which are illustrated in Figure 1(b)–(f).

Two sets of independent linear motion systems control the moving speeds of the two ends separately. The temperature of the deformation zone is elevated rapidly and limited to a specific region with the help of the induction heating system and the annular air jet cooling system. Moreover, the adjustment of process parameters and command inputs are realized by the programmable logic controller (PLC) control system, and the measuring system records the data of temperature and compression force. Concretely, the forming apparatus mainly consists of four modules, including the mechanical module, the induction heating module, the annular cooling module and the feedback control module.

2.1.2 Mechanical Module

As depicted in Figure 1(c), two push plates are separately driven by two servo motors (1 kW) cooperating with the lead screws, synchronous belts and reduction gears, to achieve high-precision movement and positioning. The two ends of a metal tube are fixed on the push plates by a three-jaw chunk and a thimble respectively, which are arranged at the center of the push plates to ensure that the compression force is concentric with the axis of the tube. The limit displacement of the push plates in this

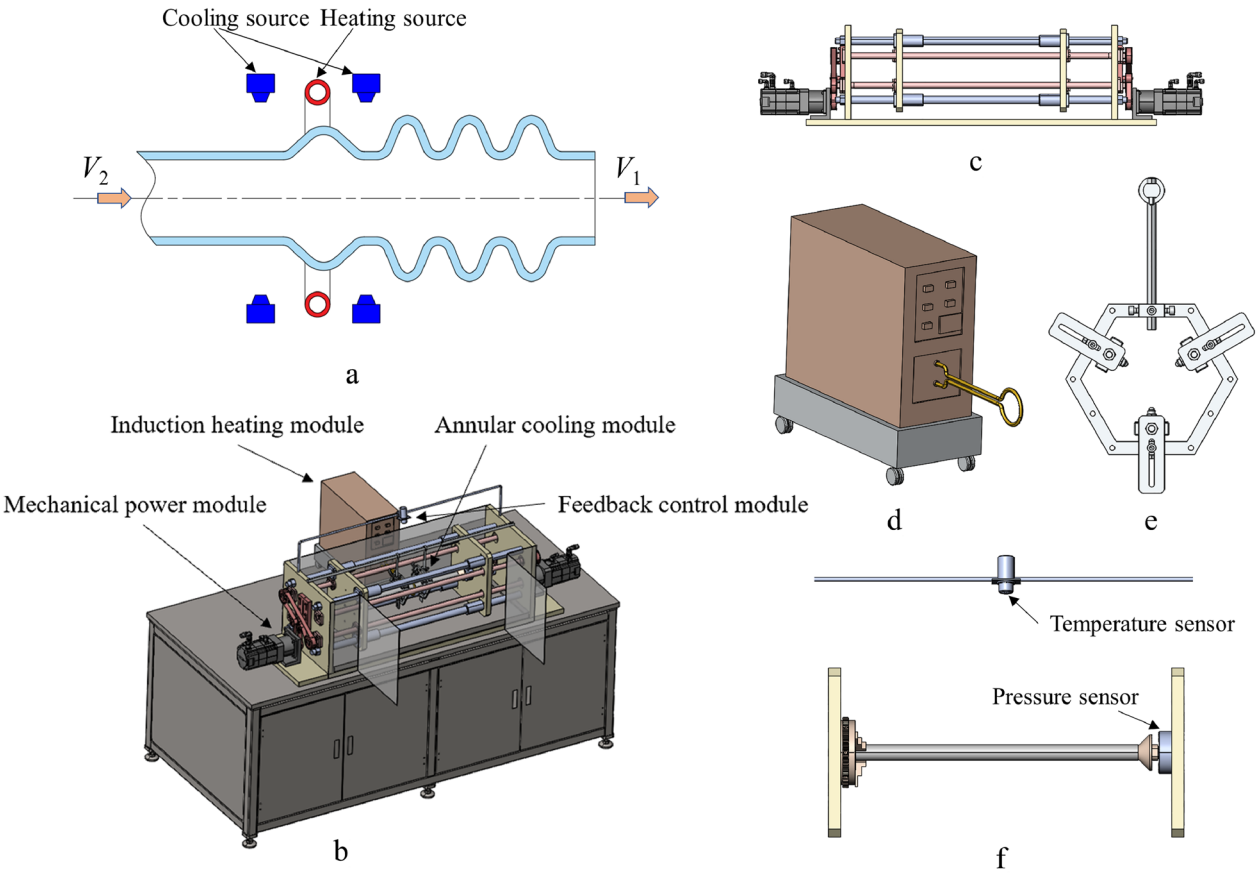

Figure 1 Schematic illustration of the forming apparatus: **a** Principle drawing, **b** Assembly drawing, **c** Mechanical module, **d** Induction heating module, **e** Annular cooling module, **f** Feedback control module

apparatus is 1.2 m and the movement speed range is 0.1–25 mm/s.

2.1.3 Induction Heating Module

As shown in Figure 1(d), a high-frequency induction heating device is employed to produce a local rapid heating area on the tube, its maximum output power is 25 kW and the frequency range is 30–100 kHz. The induction coil is replaceable so that it can meet the requirements of different heating lengths and tube diameters.

2.1.4 Annular Cooling Module

In order to limit the length of the high temperature zone, two annular cooling sources are placed adjacent to the induction coil. As shown in Figure 1(e), various nozzles are evenly arranged in a ring to ensure uniform circumferential cooling. Compressed gas or water or their mixture with different cooling effects can be injected by a high-pressure pump. And the temperature distribution along the longitudinal direction of the metal tube can be controlled by adjusting the distance between the heating coil and the coolers.

2.1.5 Feedback Control Module

An infrared thermometer is installed above the tube to capture the temperature history of the heating zone. Meanwhile, the compression force is measured by a pressure sensor fixed between the push plate and the thimble, as illustrated in Figure 1(f). In addition, a high speed 8-channel analog data acquisition card is utilized to record the values of temperature and compression force simultaneously. Through the PLC control system, different moving and heating conditions can be set and performed, and all the data measured by sensors are fed back instantly.

With the collaboration of each module, the thermal buckling forming apparatus of metal bellows has been developed, as presented in Figure 1(b). The forming process can be driven step-by-step manually or automatically.

2.2 Forming Modes

The forming apparatus is capable of producing metal bellows in two forming modes: the discontinuous bellow forming process and the continuous bellow forming process, which are respectively detailed in Section 2.2.1 and Section 2.2.2.

2.2.1 Discontinuous Bellow Forming Process

Discontinuous bellow forming process means that there is a straight tube interval between one convolution and the next. As shown in Figure 2(a), the forming steps are as follows: Step 1, the positions of the heating and cooling sources are adjusted appropriately, and the tube is heated to the target temperature at a stationary state ($V_1 = V_2 = 0$). Step 2, a proper compression speed ($V_2 > 0$) is set at the moving end and the other end is left still ($V_1 = 0$), then the axisymmetric buckling occurs and induces a convolution at the heated region where the material has been softened. Step 3, the tube is moved to the next position which is one convolution pitch away, in this step V_1 and V_2 are set to the same value. Step 4 and Step 5, the heating and buckling processes are repeated successively. Therefore, by controlling the speed variation at the two ends of the tube, a discontinuous bellow can be fabricated. The compression displacement of the moving end to form a single convolution is defined as the compression stroke, which is a key parameter of this forming process.

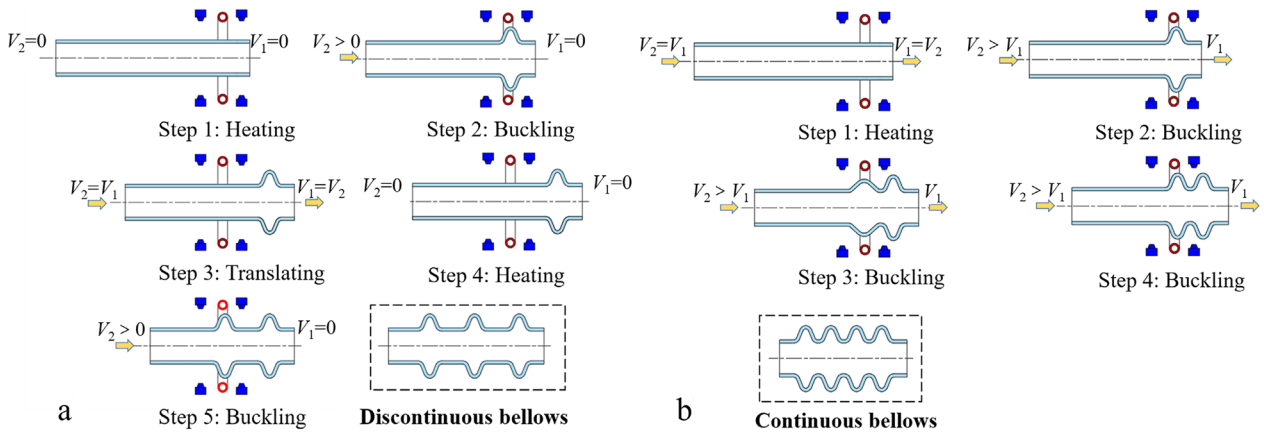

Figure 2 Schematic diagrams of thermal buckling-induced forming process: **a** Discontinuous bellow, **b** Continuous bellow

2.2.2 Continuous Bellow Forming Process

Continuous bellow forming process means that there is no straight tube interval between one convolution and the next, and all convolutions are closely arranged. This kind of bellows can also be formed by the prementioned process (Section 2.2.1), in which the translation distance should be set as the convolution width. While in this section, a more efficient process is introduced.

The forming steps are shown in Figure 2(b). Step 1, the heating and cooling sources are turned on, and their state is maintained during the whole process. Both ends of the tube are moved with an equal speed ($V_1 = V_2 > 0$), and the tube billet is heated to the predetermined temperature. Step 2, V_1 should be kept constant, and adjusted the moving speed of the other end ($V_2 > V_1$). The speed difference between the two ends induces an axial compression force to form a convolution in the softened area. Step 3, with the continuous movement of the tube, the first convolution enters the cooling area, and it will not be further compressed due to the increase in strength. Meanwhile, the temperature of the adjacent forming area is increased, and then buckling deformation develops in this region. Step 4, the second convolution is accomplished and enters the cooling area, while the temperature of the next forming area is elevated. The ratio of the speeds at the two ends during Steps 2–4 is defined as the compression ratio, which is a key parameter of this forming process.

2.3 Formed Bellows

2.3.1 Tested Material and Tube Billet

The experimental material used in this paper is 304 stainless steel with a composition of 0.043C-0.218Si-1.229Mn-0.037P-0.004S-8.213Ni-18.02Cr wt.%. The diameter and thickness of the tube billet in this test are 25 mm and 1 mm, respectively.

The elastic modulus and density of material at the default temperature of 950 ℃ are 118.2 GPa and 7.5 g·cm^{-3}, while the thermal conductivity, expansion coefficient and specific heat are 26.8 W·(m ℃)$^{-1}$, 20.5×10^{-6} ℃$^{-1}$ and 633.9 J·(kg ℃)$^{-1}$ respectively. The thermophysical and elastic parameters vary with temperature, as shown in Table 1 and Figure 3.

The hot compression tests under different temperatures have been conducted on the Gleeble-3500 test machine. The test specimens are small cylinders cut from the thick-walled tube billets. The Johnson-Cook model with the temperature term is used here to represent the mechanical properties of the material, and the final fitting form is determined as

$$\sigma_{\mathrm{Y}} = \left(291 + 2226\varepsilon_{\mathrm{p}}^{0.988}\right)\left[1 - \left(\frac{T - 298}{1375}\right)^{0.423}\right], \tag{1}$$

where σ_{Y} denotes the yield stress, ε_{p} denotes the equivalent plastic strain, and T denotes the current temperature (K).

2.3.2 Characteristics of the Formed Bellows

Figure 4 shows the pictures of the formed discontinuous and continuous bellow samples respectively. And their characteristics are discussed in this section.

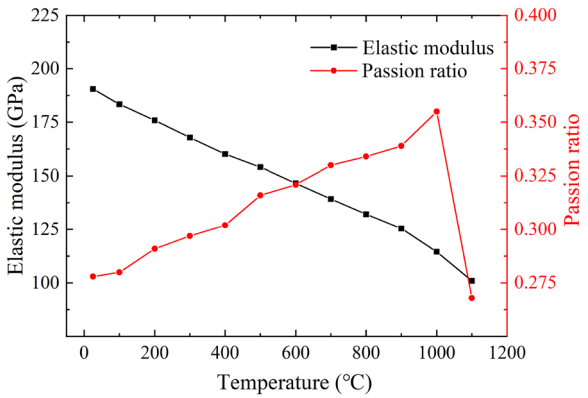

Figure 3 Elastic parameters of 304 stainless steel of different temperatures

Table 1 Thermophysical parameters of the material

Temperature T(℃)	Thermal conductivity λ(W·(m·℃)$^{-1}$)	Density ρ(g·cm^{-3})	Specific heat c(J·(kg·℃)$^{-1}$)	Expansion coefficient α($\times10^{-6}$·℃$^{-1}$)
25	14.6	7.90	462	17.0
200	16.1	7.83	512	18.0
400	18.0	7.75	540	19.1
600	20.8	7.66	577	19.6
800	23.9	7.56	604	20.2
1200	32.2	7.37	676	20.7

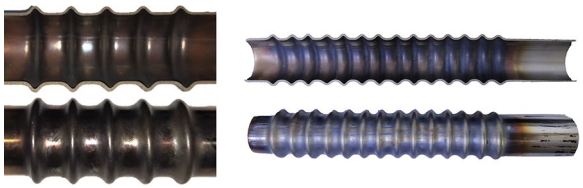

Figure 4 Formed metal bellow samples: **a** Discontinuous bellow, **b** Continuous bellow

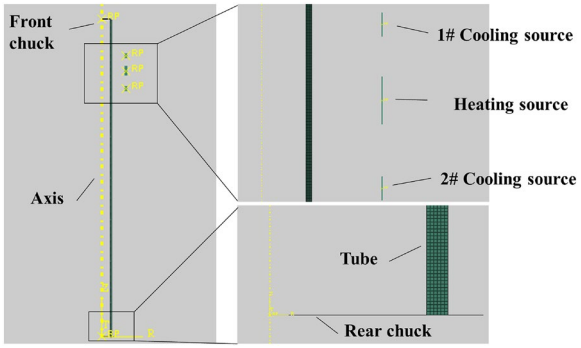

Figure 5 Schematic diagrams of FEM model

In order to form a discontinuous bellow, the tube is heated to the forming temperature of 950 °C, then the compression stroke of 3 mm and the translation distance of 15 mm are recycled to produce convolutions one by one. A bellow sample with 5 convolutions is formed as shown in Figure 4(a). It has a configurational symmetry in the circumferential direction. Furthermore, the shape profiles of the five convolutions are quite similar, and the variation range of convolution height and convolution width is no more than 5%. Figure 4(b) shows a continuous bellow sample, which is formed with a compression ratio of 1.6 ($V_2=0.7$ mm/s and $V_1=0.5$ mm/s), and the forming temperature is set as 950 °C, same as that for the discontinuous bellow. And it is revealed from Figure 4(b) that the continuous bellow also has good uniformity and stability in its convolution profile.

At present, the forming precision of the new process is controlled through the response surface method (RSM). Specifically, based on RSM, the expected convolution profile can be formed by the joint control of the compression stroke, heating temperature, heating width and other factors. More details on the forming precision of the thermal buckling-induced forming process can be found in Ref. [25].

3 Forming Simulation

3.1 FEM Modelling

The finite element model has been established on the ABAQUS platform to get a clear inspection of the deformation mechanism of the thermal buckling forming process. According to the geometrical feature and its deformation way, an axisymmetric FEM model is established, as shown in Figure 5. The size of the original tube billet is 25 mm in diameter and 1 mm in thickness.

The model mainly consists of four parts, including the fixture chuck, heating source, cooling sources and tube billet. The lengths of the heating and cooling sources are set as the actual values, as well as their distances. For simplification, the induction heating source is represented by a coil with a given heating flux, and the cooling sources are represented by coils with a given heat dissipation coefficient. Such simplification must obey the rule of temperature equivalence, i.e., the equivalent heating flux and heat dissipation coefficient are determined by using the reverse calculation based on FEM simulations and the following two experiments:

(i) The induction heating source is turned on while the cooling sources are turned off. And the tube is heated until the temperature of the center point reaches 950 °C. Then the heating source is turned off and the tube is naturally cooled to room temperature. The temperature data of the center point during the process are recorded.
(ii) The heating source and the cooling sources are turned on. And the tube is heated until the temperature of the center point reaches 950 °C. Then the heating source is turned off and the tube is cooled to room temperature under the action of the cooling sources. The temperature data of the center point during the process are recorded.

Through the comparison of FEM results and the above experimental results, the equivalent heating flux and the forced heat dissipation coefficient are determined by reverse calculation. Specifically, the temperature data of (i) are used to fit the equivalent heating flux because the cooling sources are turned off in this condition and the forced heat dissipation can be ignored. Then the temperature data of (ii) are used to fit the forced heat dissipation coefficient since the equivalent heating flux is known. Ultimately, the equivalent heating flux and the forced heat dissipation coefficient are determined as $H_f=500000$ J·(s·m^2)$^{-1}$ and $D_f=250$ W·(m^2·K)$^{-1}$, respectively.

Without loss of generality, the fixture chucks are set as rigid bodies. In order to accurately simulate the clamping way of the three-jaw chuck and the thimble in the experiment, one end of the tube is restrained with the chuck by

Tie Constraint and the hard friction contact condition is adopted at the other end.

The stainless steel is considered as a thermal-elastic-plastic material, where the Von Mises yield criterion and isotropic hardening model are used in the simulation. The four-node coupled thermal-mechanical axisymmetric element with reduction integration (CAX4RT) is used for the tube billet, and the model has been divided into 6 layers of elements in the thickness direction.

3.2 Verification of the FEM Model

The convolution height and the wall thickness at the crest are selected as indicators to verify the FEM model. As soon as the measuring point on the tube is heated to 950 ℃, the tube is compressed by the push plates and then a convolution is produced. After that, the heating source is turned off and the tube is cooled to room temperature. The experiment is repeated three times to obtain the mean values. The outer diameter of the bellow at the convolution crest has been measured and then the experimental data of the convolution height can be obtained by simple data processing. After that, the bellow is cut along the axis (as shown in Figure 4), and then the wall thickness at the crest can be measured. The above measurement is conducted by the digital vernier caliper with a resolution of 0.01 mm and an error of ±0.02 mm. And the simulation is completely consistent with the experimental condition. As depicted in Figure 6(a), the value of convolution height increases with the augmentation of the compression stroke, keeping a linear relationship approximately. It can be observed that the simulated convolution height fits the experimental one quite well with a relative error of less than 5%. As shown in Figure 6(b), the wall thickness at the convolution crest is basically maintained at 1.1–1.2 mm, and the simulated wall thickness is slightly smaller than the experimental data. Therefore, the reliability of the FEM model is basically verified by the evaluation of the convolution height and the wall thickness at the crest.

3.3 Analysis of the Convolution Profile

In this section, the simulated convolution profile is analyzed, and the wall thickness and the uniformity of convolution heights are taken as indicators to reflect the quality of bellows. High forming quality usually refers to the small thickness reduction and the small difference between the convolution heights.

Figure 7(a) shows the convolution height and wall thickness distribution of the discontinuous bellow along the axial direction. It can be found that all thickness values are larger than that of the original tube billet, which means the wall thinning that appears in other forming methods doesn't exist in this test. It is also found that the thickness of each convolution profile is distributed in the shape of an "epsilon" glyph, and the convolution crest has the maximum thickening rate, i.e., 9%. The heights of different convolutions almost keep consistent (i.e., the variation range is less than 5%). In addition, the maximum load (corresponding to the critical buckling load) is only about 4500 N in this test, which is much smaller than that in hydroforming or other bellow forming processes, so its forming force can be provided by a simple small servo motor.

Figure 7(b) depicts the convolution height and thickness distribution of the continuous bellow. It is noted that the convolution height of the first convolution is greater

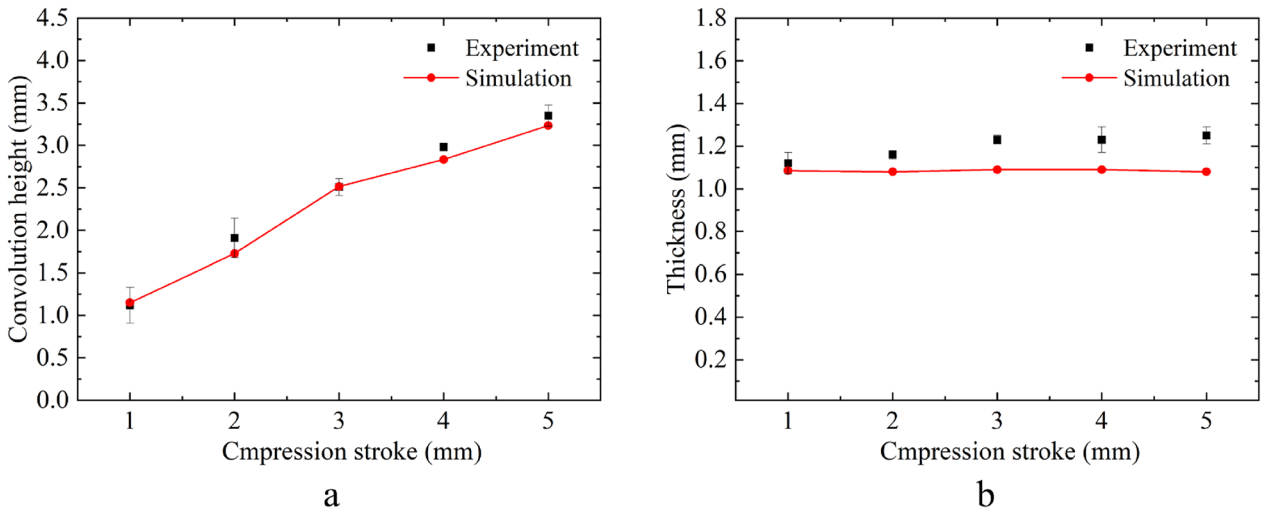

Figure 6 Comparison of simulation results and experimental data: **a** Convolution height and **b** Wall thickness at the convolution crest

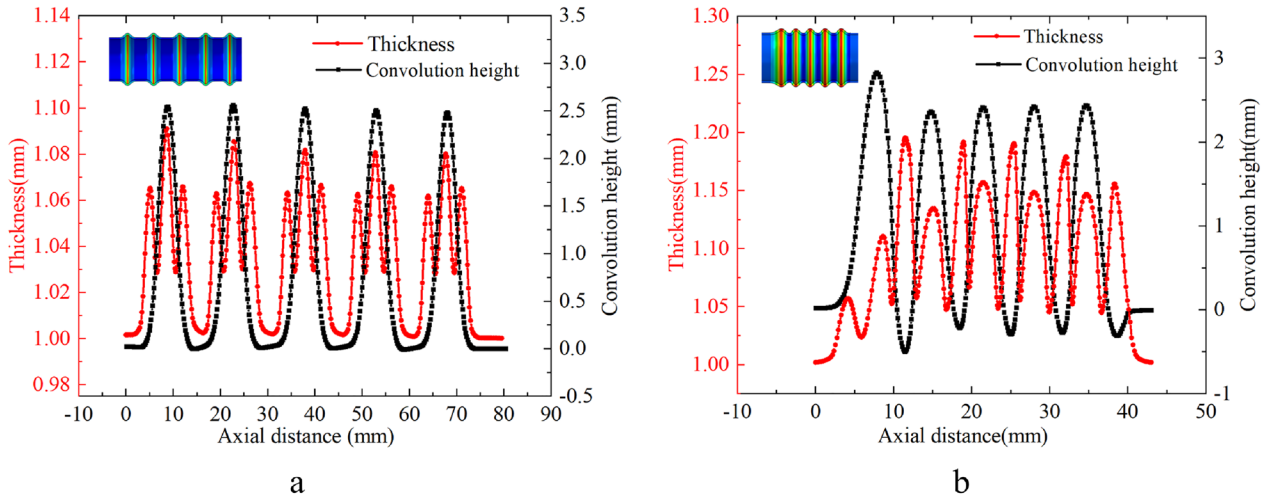

Figure 7 **a** Curves of wall thickness and convolution height of the discontinuous bellow, **b** Curves of wall thickness and convolution height of the continuous bellow

than others. That is because the tube is in a static state at the beginning of compression and then converted to the moving state in the subsequent forming process, which causes the high temperature area to be offset by a certain distance. While after that, the forming process keeps stable and the subsequently formed convolutions are uniform. Furthermore, the continuous bellow has a certain degree of concave at the convolution trough, which is manifested by the value of height below 0. This phenomenon doesn't appear in the forming of discontinuous bellows. The reason is that during the thermal buckling of continuous bellows, the high temperature zone of the tube moves continuously. And in the later stage of forming a convolution, the high temperature zone is located near the convolution trough and the material in this area will flow inward during the subsequent compression, resulting in the increase of convolution depth.

In addition, it can be observed from Figure 7 that there is an apparent difference in wall thickness distribution between the two types of bellows. The maximum wall thickness appears at the convolution crest for the discontinuous bellow while it appears at the convolution trough for the continuous bellow. The thickness distribution of the latter is more like the letter "W". However, it should be noted that the thickness at any position of the continuous bellow is still greater than that of the original tube billet.

4 Influence of Forming Parameters

In this section, the effects of the process parameters (compression stroke, heating length and heating temperature) and the geometric parameters (tube thickness and diameter) are discussed based on FEM simulations of the discontinuous bellow forming process. All the studied parameters are listed in Table 2, where the values with bracket are considered as the default values in this experiment. A single convolution is formed during the process, and the parameter effects on the convolution height and the wall thickness are investigated, where the wall thickness is also considered as an indicator to evaluate the quality of the formed bellows.

4.1 Effects of Process Parameters

4.1.1 Compression Stroke

The compression stroke is a key process parameter that directly affects the profile of convolution. The profile data of the formed convolution under different compression strokes are shown in Figure 8(a). The convolution height increases with the augmentation of compression stroke and shows a linear relationship approximately. Meanwhile, the compression stroke has a weak influence on the wall thickness as shown in the red line of Figure 8(a), and the wall thickness at the convolution crest stays in a small range of 1.08–1.09 mm. For the studied bellow forming process, the plastic deformation occurs before buckling deformation, and the wall thickness increases

Table 2 Values of the forming parameters

Parameters	Value
Compression stroke *L*(mm)	2, (3), 4, 5
Heating length *w*(mm)	8, 10, (12),14
Heating temperature *T*(℃)	850, (950), 1050, 1150
Initial wall thickness *t*(mm)	0.8, (1), 1.2, 1.5
Diameter *d*(mm)	15, (25), 35, 45

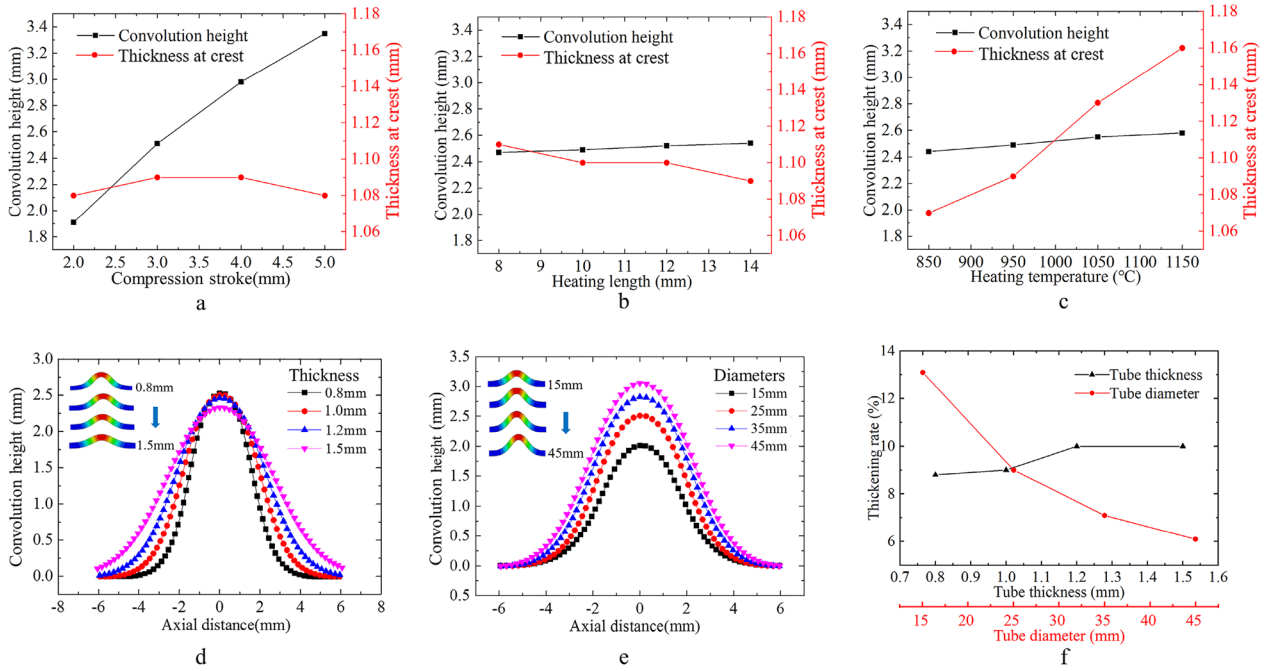

Figure 8 Curves of convolution profile at: **a** different compression strokes, **b** different heating lengths, **c** different heating temperatures, **d** different initial tube wall thicknesses, **e** different tube diameters, and **f** thickening rate at different geometric parameters

at this stage within a quite small compression stroke. After that, the post-buckling flow occurs and the main deformation behavior is the bending deformation. Thus, the contribution of the compression stroke is mainly to increase the bending deflection of the tube billet, i.e., the convolution height.

4.1.2 Heating Length

The heating length determines the temperature distribution of the tube, and further affects the buckling deformation region. Figure 8(b) shows the convolution height and convolution thickness at the crest under different heating lengths (8 mm, 10 mm, 12 mm and 14 mm). The convolution height gradually rises with the increase of heating length, while the wall thickness presents an opposite law with a slight decline.

The augmentation of heating length increases the buckling deformation area, and then results in a higher convolution height at the same compression stroke. However, the larger high temperature zone also reduces the critical buckling value, which means the pure plastic deformation stage is shortened and the wall thickening is weakened.

4.1.3 Heating Temperature

The heating temperature affects not only the temperature distribution of the tube, but also the plastic flow behavior of the material. Figure 8(c) shows the convolution height and crest thickness under different heating temperatures (850 °C, 950 °C, 1050 °C and 1150 °C). It is demonstrated that the thickness at the convolution crest increases significantly with the augmentation of heating temperature, and the effect is much more apparent than that of compression stroke and heating length.

Besides, there is a slight positive correlation between convolution height and heating temperature. The convolution heights at different heating temperatures are close to each other, of which the variation range is less than 6%.

4.2 Effects of Geometric Parameters

The initial tube diameter and wall thickness are the two main geometric parameters for the tube billet. Their effects on the final bellows are analyzed, where the wall thicknesses are chosen as 0.8 mm, 1 mm, 1.2 mm and 1.5 mm, and the initial diameters are chosen as 15 mm, 25 mm, 35 mm and 45 mm, respectively.

Figure 8(d) and (e) shows the convolution height and width at different geometric parameters. When the initial wall thickness increases, the convolution height diminishes and the width increases. However, the increase in tube diameter leads to the augmentation of both convolution height and width. The reasons can be summarized as follows:

The increase of initial wall thickness results in a larger critical buckling value, which means that the plastic deformation course increases, and the post-buckling deformation course is shortened, leading to the decrease

of the convolution height and the increase of plastic thickening, as shown in Figure 8(d) and (f). And the large wall thickness makes it difficult for local deformation to develop, so the convolution width increases. On the other hand, the increase in tube diameter means that the critical buckling value decreases, shortening the plastic deformation course and increasing the post-buckling deformation course, which leads to the decrease of the thickening rate and the augmentation of the convolution height, as shown in Figure 8(e) and (f).

5 Conclusions

The present study focuses on the controllable buckling deformation of metal bellow forming. Through reasonable allocations of the technological parameters, the buckling deformation can be used as an effective forming method for metal bellows with attractive advantages. The conclusions are as follows:

(1) The compression stress is the major engine during the thermal buckling forming process, which leads to remarkable improvements in lower forming force, better material flowability and higher forming limit. Furthermore, there is no obvious thickness thinning in the formed bellows, which gives them a better energy absorption performance.

(2) Both discontinuous bellows and continuous bellows can be produced by the thermal buckling forming process. The convolution profile uniformity of discontinuous bellows is favorable, of which the wall thickness is distributed in the shape of an "epsilon" glyph, and the maximum thickness appears at the convolution crest. The curve of the wall thickness distribution of continuous bellows is in the shape of a "W" glyph, which has the largest value at the convolution trough.

(3) Compression stroke, heating length and heating temperature have different degrees of positive correlation with the convolution height. The increase in wall thickness leads to lower convolution height, higher convolution width and higher thickening rate, but the initial diameter shows an opposite law.

It also should be noted that the presented buckling-induced forming method still needs further studies. One of the main shortcomings is that its forming precision is not as good as that of die-forming methods, which we believe can be improved by tool assistance and some work is ongoing.

Acknowledgements
We thank Mr. Ziqi Ding and Mr. Jun Liu for their support and previous work.

Author contributions
TX was in charge of the experiments and simulations; DL and TZ assisted in the experiments and data analyses; XH and YS checked and improved the manuscript in writing. All authors read and approved the final manuscript.

Authors' information
Tianyin Zhang is currently a PhD candidate at *School of Materials Science and Engineering, Shanghai Jiao Tong University, China*.
Dongqing Li is currently an engineer at *Hangzhou Steam Turbine & Power Group Co., Ltd., China*.
Tianjiao Xu is a graduate student of *School of Materials Science and Engineering, Shanghai Jiao Tong University, China*.
Yongfeng Sui is a professor-level senior engineer at *Hangzhou Steam Turbine & Power Group Co., Ltd., China*.
Xianhong Han is currently a professor at *School of Materials Science and Engineering, Shanghai Jiao Tong University, China*. His research focuses on hot stamping technology.

Funding
Supported by National Natural Science Foundation of China (Grant No. 52175349), and Aeronautical Science Foundation of China (Grant No. 20200009057004).

Availability of data and materials
The datasets supporting the conclusions of this article are included within the article.

Competing interests
The authors declare that they have no competing interests.

Received: 20 October 2021 Revised: 2 November 2022 Accepted: 31 January 2023
Published online: 10 February 2023

References

[1] J Liu, H Li, Y Liu, et al. "Size effect" related hydroforming characteristics of thin-walled 316-L bellow considering pressure change. *International Journal of Advanced Manufacturing Technology*, 2018, 98(1–4): 505–522.
[2] Z Yuan, S Huo, J Ren. Mathematical description and mechanical characteristics of reinforced S-shaped bellows. *International Journal of Pressure Vessels and Piping*, 2019, 175: 103931.
[3] Z Hao, J Luo, L Chen, et al. Failure mechanism of unequal parameters metal bellows under repeated bending process. *Engineering Failure Analysis*, 2021, 129: 105671.
[4] X Nan, Z J Wang, J Yi, et al. Controlling of material flow in the quasi-bulk forming of thin-walled corrugated rings through optimization of contact pressure. *International Journal of Advanced Manufacturing Technology*, 2017, 91(5–8): 2077–2088.
[5] A Alaswad, K Y Benyounis, A G Olab. Tube hydroforming process: A reference guide. *Materials & Design*, 2012, 3: 328–339.
[6] S W Lee. Study on the forming parameters of the metal bellows. *Journal of Materials Processing Technology*, 2002, 130–131(11): 47–53.
[7] G Faraji, M K Besharati, M Mosavi, et al. Experimental and finite element analysis of parameters in manufacturing of metal bellows. *International Journal of Advanced Manufacturing Technology*, 2008, 38(7–8): 641–648.
[8] M Zhan, F Shi, Q Deng, et al. Forming mechanism and rules of mandreless neck-spinning on corrugated pipes. *Journal of Plasticity Engineering*, 2014, 21(2): 108–115. (in Chinese)
[9] X Shi, Y Li, M Yang, et al. Investigation on deformation characteristics of internal spinning incremental forming process for metal corrugated tubes. *Forging & Stamping Technology*, 2018, 43(2): 55–61. (in Chinese)
[10] J Yang, G Wang, T Zhao, et al. Study on the experiment and simulation of titanium alloy bellows via current-assisted forming technology. *JOM*, 2018, 70(7): 1118–1123.
[11] Z J Wang, N Xiang, J Yi, et al. Forming thin-walled circular rings with corrugated meridians via quasi-bulk deformation of metal blank and viscous medium. *Journal of Materials Processing Technology*, 2016, 236: 35–47.

[12] P M Reis. A perspective on the revival of structural (in) stability with novel opportunities for function: From buckliphobia to buckliphilia. *Journal of Applied Mechanics-Transactions of the ASME*, 2015, 82(11): 1–4.
[13] W Borchani, P Jiao, R Burgueño, et al. Control of postbuckling mode transitions using assemblies of axially loaded bilaterally constrained beams. *Journal of Engineering Mechanics*, 2017, 143(10): 04017116.
[14] S O Erbil, U Hatipoglu, C Yanik, et al. Full electrostatic control of nanomechanical buckling. *Physical Review Letters*, 2020, 124(4): 1–19.
[15] H Zhao, K Li, M Han, et al. Buckling and twisting of advanced materials into morphable 3D mesostructures. *Proceedings of the National Academy of Sciences of the United States of America*, 2019, 116(27): 13239–13248.
[16] S J Yuan, W Yuan, X Wang. Effect of wrinkling behavior on formability and thickness distribution in tube hydroforming. *Journal of Materials Processing Technology*, 2006, 177(1–3): 668–671.
[17] L M Alves, P A F Martins. Mechanical joining of tubes to sheets along inclined planes. *Steel Research International*, 2012, 83(12): 1135–1140.
[18] S Supriadi, N Q Hung, T Furushima, et al. A novel dieless bellows forming process using local heating technique. *10th International Conference on Technology of Plasticity*, Aachen, Germany, 2011: 950–955.
[19] T Furushima, N Q Hung, K I Manabe, et al. Development of semi-dieless metal bellows forming process. *Journal of Materials Processing Technology*, 2013, 213(8): 1406–1411.
[20] Z C Zhang, K-i Manabe, T Furushima, et al. Development of dieless metal bellows forming process with local heating technique. *Proceedings of the Institution of Mechanical Engineers, Part B: Journal of Engineering Manufacture*, 2015, 229(4): 664–669.
[21] M Sedighi, M Shamsi. A new approach in producing metal bellows by local arc heating: a parametric study. *International Journal of Advanced Manufacturing Technology*, 2017, 93(9–12): 3211–3219.
[22] J Liu, Z Lv, Y Liu, et al. Deformation behaviors of four-layered U-shaped metallic bellows in hydroforming. *Chinese Journal of Aeronautics*, 2020, 33(12): 3479–3494.
[23] B H Kang, M Y Lee, S M Shon, et al. Forming various shapes of tubular bellows using a single-step hydroforming process. *Journal of Materials Processing Technology*, 2007, 194(1–3): 1–6.
[24] T Zhang, M Liu, X Han. A non-associated flow rule with simple non-branching form representing the apparent non-normality effects after abrupt strain-path change. *International Journal of Plasticity*, 2022, 159: 103452.
[25] T Xu, T Zhang, X Han. Analysis on process parameters of thermal buckling forming for aluminum alloy bellows based on response surface method. *Suxing Gongcheng Xuebao/Journal of Plasticity Engineering*, 2022, 29(9): 69–79. (in Chinese)